

Configuration and stereodynamics of *exolendo*-isomeric push-pull alkenes of pentadiene structure

PERKIN
2

Erich Kleinpeter,^{*,a} Matthias Heydenreich,^a Jochen Woller,^a Gunter Wolf,^a Andreas Koch,^a Gerhard Kemper^a and Kalevi Pihlaja^b

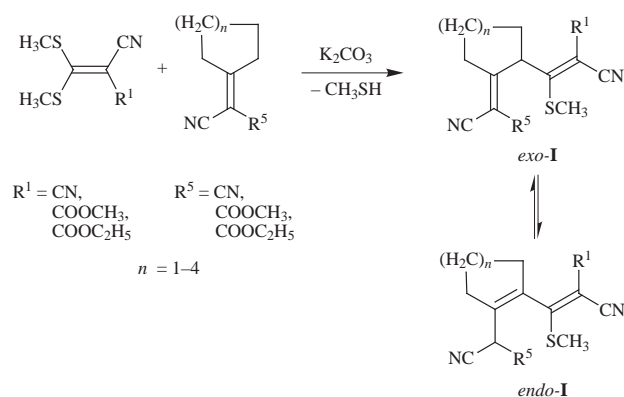
^a Institut für Organische Chemie und Strukturanalytik, Universität Potsdam, Am Neuen Palais 10, D-14469 Potsdam, Germany

^b Department of Chemistry, University of Turku, FIN-20500 Turku, Finland

The configuration of the two double bonds in a series of alkenyl-substituted cyclic push-pull pentadienes [-1,3- (1–9, endocyclic) and -1,4-dienes (1–9, exocyclic)], the corresponding preferred ground state conformations and the stereodynamics were studied by the whole arsenal of 1D and 2D NMR spectroscopic methods, mass spectrometry and parallel molecular modelling. The configuration was found strongly dependent on the ring size (five-, six-, seven- and eight-membered). The dynamic phenomena found in the ¹H and ¹³C NMR spectra were proved to result from the sterically hindered rotation about the C2–C3 bond; the torsional barriers were determined by dynamic NMR spectroscopy and also estimated by semi-empirical and *ab initio* quantum chemical calculations.

Introduction

Cycloalkylidenemalononitriles (R⁵ = CN) and the corresponding malonic esters (R⁵ = COOMe, COOEt) react readily with ketene-*S,S*-acetals in the presence of a base (e.g. K₂CO₃) giving a number of spectroscopically interesting push-pull pentadienes **1** (cf. Scheme 1).¹ The two C,C double bonds can be in



Scheme 1

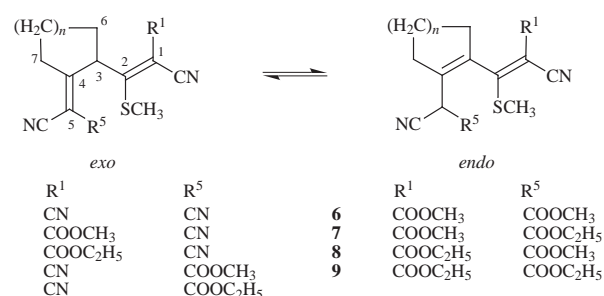
the 1,3- (endocyclic) or 1,4-positions (exocyclic); the ratio of the two isomers was found to be strongly dependent on the ring size ($n = 1, 2, 3, 4$) of the push-pull pentadienes **1**. In a number of cases, more than two sets of signals were present in the NMR spectra, indicating further isomerism and/or temperature dependent stereodynamics (some lines in both the ¹H and ¹³C NMR spectra of the five-membered ring compounds were found to be exchange-broadened).

The main objectives of this paper are (i) to assign the *exolendo* isomerism, (ii) to prove the ground state conformations, (iii) to identify the stereodynamic behaviour and (iv) to quantify the push-pull character of the *exolendo* pentadienes **1** studied.

Results and discussion

Assignment of the ¹H and ¹³C NMR spectra

The ¹H NMR spectra of the push-pull pentadienes studied (cf. Scheme 2) are fairly simple for the stereochemically/



Scheme 2

electronically interesting part of these molecules: S–Me and the two substituents R¹ and R⁵ show very characteristic absorptions (S–Me as sharp singlets at $\delta = 2.20$ – 2.70 and ca. 2.90 for **1** ($n = 3$, *exo*) and **1** ($n = 4$, *exo*), respectively; COOCH₂CH₃; $\delta = 4.20$ – 4.30 and 1.30 – 1.40 , respectively; COOCH₃; $\delta = 3.80$ – 3.90), the signals of H5 in the *endo*-isomers (generally as a singlet at $\delta = 4.20$ – 4.70) and H3 in the *exo*-isomers (also between 4 and 5 ppm) are often overlapped by the resonances of the additional ester functions. When not overlapped, the H3 protons were found to give a multiplet of the AB(C)X type. The other ring protons show complicated multiplets which were not analyzed since they are not relevant to this study. Using the resonances of the unequivocally assigned protons mentioned above, the carbon resonances could be assigned unambiguously via C,H COSY NMR experiments with inverse detection by determining direct C,H (HMQC) and long-range C,H connectivities (HMBC). Only the various nitrile resonances could not be assigned unambiguously due to the lack of nearby protons; otherwise the assignment of the ¹H and ¹³C chemical shifts given for the *exo*- (cf. Tables 1 and 2) and *endo*-isomers (cf. Tables 3 and 4) of the studied push-pull pentadienes **1**–**9** is complete.

Below their coalescence temperatures all compounds show two sets of signals corresponding to the two rotamers of the alkene substituent.

exolendo-Isomerism of the push-pull pentadienes 1–9

The corresponding assignment should be simple based on the H–H coupling pattern of H3 in the *exo*- and that of H5 in the *endo*-isomers. Unfortunately, the corresponding resonances are

Table 1 ^1H NMR spectra (δ) of *exo*-isomers **1**, **4** and **5** (solvent CDCl_3 -TMS)

	H-3	Remaining ring-H	R ⁵	SCH ₃
1 (<i>n</i> = 2, <i>exo</i>)	4.15 (dd, 1H)	1.60–3.07 (m, 8H)	—	2.97 (s, 3H)
1 (<i>n</i> = 3, <i>exo</i>)	4.31 (dd, 1H)	1.15–3.28 (m, 10H)	—	2.90 (s, 3H)
1 (<i>n</i> = 4, <i>exo</i>)	4.29 (dd, 1H)	0.95–3.11 (m, 12H)	—	2.92 (s, 3H)
4 (<i>n</i> = 1, <i>exo</i>)	4.53 (t, 1H)	1.78–3.07 (m, 6H)	3.86 (s, 3H)	2.78 (s, 3H)
5 (<i>n</i> = 1, <i>exo</i>)	4.52 (t, 1H)	1.78–3.08 (m, 6H)	4.32 (q, 2H) 1.36 (t, 3H)	2.78 (s, 3H)

Table 2 ^{13}C NMR spectra (δ) of *exo*-isomers **1**, **4** and **5** (solvent CDCl_3 -TMS)

	C1	C2	C3	C4	C5	Remaining ring-C	R ¹	R ⁵	CN	SCH ₃
1 (<i>n</i> = 2, <i>exo</i>)	87.0	179.5	50.9	178.0	81.6	22.1; 24.2; 31.6; 34.2	111.9	110.7	110.8; 111.0	18.4
1 (<i>n</i> = 3, <i>exo</i>)	90.5	180.4	53.8	183.1	80.8	27.8; 29.6; 29.8; 33.1; 36.6	110.8	110.6	111.8; 111.9	17.9
1 (<i>n</i> = 4, <i>exo</i>)	90.2	180.6	53.2	184.9	80.2	24.7; 25.4; 29.1; 29.8; 31.6; 34.6	111.4	110.6	111.8; 112.5	18.2
4 (<i>n</i> = 1, <i>exo</i>)	77.8	184.5	51.8	179.4	104.9	24.1; 35.6; 38.9	112.3	161.1 (CO) 53.1 (OCH ₃)	112.4; 114.2	17.2
5 (<i>n</i> = 1, <i>exo</i>)	77.9	184.8	5.17	179.9	105.3	24.1; 35.6; 38.8	111.4	160.7 (CO) 64.0 (OCH ₂) 14.0 (CH ₃)	112.4; 114.2	17.2

Table 3 ^1H NMR spectra (δ) of *endo*-isomers **1–9** (solvent CDCl_3 -TMS)

	H5	Remaining ring-H	R ¹	R ⁵	SCH ₃
1 (<i>n</i> = 2, <i>endo</i>)	4.59 (s, 1H)	1.60–3.07 (m, 8H)			2.52 (s, 3H)
2 (<i>n</i> = 2, <i>endo</i>)	4.70 (s, 1H)	1.71–2.52 (m, 8H)	3.86 (s, 3H)		2.28 (s, 3H)
2 (<i>n</i> = 3, <i>endo</i>)	4.21 (s, 3H)	1.68–2.53 (m, 10H)	3.82 (s, 3H)		2.41 (s, 3H)
	4.30 (s, 3H)		3.86 (s, 3H)		2.46 (s, 3H)
	4.38 (s, 3H)		3.87 (s, 3H)		2.53 (s, 3H)
2 (<i>n</i> = 4, <i>endo</i>)	4.20 (s, 1H)	1.49–2.55 (m, 12H)	3.80 (s, 3H)		2.41 (s, 3H)
3 (<i>n</i> = 2, <i>endo</i>)	4.71 (s, 1H)	1.70–2.40 (m, 8H)	4.25 (q, 2H) 1.29 (t, 3H)		2.26 (s, 3H)
3 (<i>n</i> = 3, <i>endo</i>)	4.22 (s, 3H)	1.64–2.75 (m, 10H)	4.29 (q, 2H) 1.37 (t, 3H)		2.40 (s, 3H) 2.48 (s, 3H) 2.53 (s, 3H)
	4.30 (s, 3H)				
	4.38 (s, 3H)				
3 (<i>n</i> = 4, <i>endo</i>)	4.28 (s, 1H)	1.44–2.52 (m, 12H)	4.28 (q, 2H) 1.38 (t, 3H)		2.41 (s, 3H)
4 (<i>n</i> = 2, <i>endo</i>)	4.29 (s, 1H)	1.61–2.40 (m, 8H)		3.75 (s, 3H)	2.40 (s, 3H)
	4.30 (s, 1H)			3.76 (s, 3H)	2.46 (s, 3H)
4 (<i>n</i> = 3, <i>endo</i>)	4.28 (s, 1H)	1.70–2.50 (m, 10H)		3.89 (s, 3H)	2.49 (s, 3H)
	4.31 (s, 1H)			3.92 (s, 3H)	2.50 (s, 3H)
4 (<i>n</i> = 4, <i>endo</i>)	4.37 (s, 1H)	1.49–2.60 (m, 12H)		3.85 (s, 3H)	2.48 (s, 3H)
	4.40 (s, 1H)			3.87 (s, 3H)	2.52 (s, 3H)
5 (<i>n</i> = 2, <i>endo</i>)	5.05 (s, 1H)	1.71–2.29 (m, 8H)		4.23 (q, 2H)	2.53 (s, 3H)
	5.11 (s, 1H)			1.24 (t, 3H)	2.60 (s, 3H)
5 (<i>n</i> = 3, <i>endo</i>)	4.25 (s, 1H)	1.65–2.54 (m, 10H)		4.34 (q, 2H)	2.50 (s, 3H)
	4.27 (s, 1H)			1.35 (t, 3H)	2.51 (s, 3H)
				1.36 (t, 3H)	
5 (<i>n</i> = 4, <i>endo</i>)	4.32 (s, 1H)	1.68–2.52 (m, 12H)		4.32 (q, 2H) 1.38 (t, 3H)	2.48 (s, 3H) 2.52 (s, 3H)
6 (<i>n</i> = 1, <i>endo</i>)	4.31 (s, 1H)	1.70–2.86 (m, 6H)	3.85 (s, 3H)	3.86 (s, 3H)	2.36 (s, 3H)
	4.39 (s, 1H)				2.42 (s, 3H)
6 (<i>n</i> = 3, <i>endo</i>)		1.66–2.50 (m, 10H)	3.89 (s, 3H)	3.83 (s, 3H)	2.38 (s, 3H) 2.45 (s, 3H)
6 (<i>n</i> = 4, <i>endo</i>)	4.40 (s, 1H)	1.49–2.61 (m, 12H)	3.84 (s, 3H)	3.87 (s, 3H)	2.27 (s, 3H)
	4.43 (s, 1H)		3.85 (s, 3H)	3.88 (s, 3H)	2.36 (s, 3H)
7 (<i>n</i> = 1, <i>endo</i>)	4.30 (s, 1H)	2.50–2.81 (m, 6H)	3.86 (s, 3H)	4.30 (q, 2H) 1.30 (t, 3H)	2.35 (s, 3H)
7 (<i>n</i> = 3, <i>endo</i>)	4.26 (s, 1H)	1.63–2.60 (m, 10H)	3.82 (s, 3H) 3.86 (s, 3H)	4.26 (q, 2H) 1.37 (t, 3H)	2.34 (s, 3H) 2.40 (s, 3H)
			3.87 (s, 3H)	4.30 (q, 2H)	2.28 (s, 3H)
7 (<i>n</i> = 4, <i>endo</i>)	4.38 (s, 1H)	1.53–2.60 (m, 12H)	3.88 (s, 3H)	4.32 (q, 2H) 1.34 (t, 3H) 1.36 (t, 3H)	2.36 (s, 3H)
	4.41 (s, 1H)				
8 (<i>n</i> = 1, <i>endo</i>)	4.35 (s, 1H)	1.70–2.83 (m, 6H)	4.31 (q, 2H) 1.37 (t, 3H)	3.86 (s, 3H)	2.35 (s, 3H) 2.41 (s, 3H)
	4.40 (s, 1H)				
8 (<i>n</i> = 3, <i>endo</i>)	4.30 (s, 1H)	1.63–2.57 (m, 10H)	4.29 (q, 2H) 1.36 (t, 3H)	3.83 (s, 3H) 3.86 (s, 3H)	2.32 (s, 3H) 2.38 (s, 3H)
			4.30 (q, 2H)	3.83 (s, 3H)	2.28 (s, 3H)
8 (<i>n</i> = 4, <i>endo</i>)	4.41 (s, 1H)	1.49–2.57 (m, 12H)	1.38 (t, 3H)	3.87 (s, 3H)	2.35 (s, 3H)
	4.44 (s, 1H)				
9 (<i>n</i> = 1, <i>endo</i>)	4.32 (s, 1H)	2.17–2.81 (m, 6H)		4.32 (q, 4H) 1.32 (t, 6H)	2.41 (s, 3H)
9 (<i>n</i> = 3, <i>endo</i>)	4.26 (s, 1H)	1.64–2.55 (m, 10H)		4.26 (m, 4H) 1.35 (m, 6H)	2.34 (s, 3H) 2.39 (s, 3H)
				4.27 (q, 4H)	2.33 (s, 3H)
9 (<i>n</i> = 4, <i>endo</i>)	4.30 (s, 1H)	1.66–2.53 (m, 12H)		1.36 (t, 6H)	2.38 (s, 3H)
	4.33 (s, 1H)				

very close to each other (δ ca. 4–5) and, additionally, overlap with the signals of the ester CH_2 group. However, where the coupling pattern of these two protons could be solved, H5 in the *endo*-isomers proved to be, in general, a singlet and H3 in the *exo*-isomers was further split into a multiplet due to coupling to the adjacent ring protons. Only the major isomers (in the case of the six-membered ring both isomers) were assigned in this way and both their ^1H and ^{13}C chemical shifts are listed in Tables 1–4; sometimes the second isomer was found to be present in the gas phase from the EI mass spectra² although the second set of signals could not be found from the solution NMR spectra.

As another criterion for the *exo/endo*-isomerism of the $\text{C}=\text{C}$ double bond, the marked π -electron alternation of the *exo* $\text{C}4=\text{C}5$ double bond [$\Delta\delta(\text{C}4=\text{C}5) > 74.6$, characteristic push-pull effect] was considered; in contrast, the *endo* $\text{C}3=\text{C}4$ double bond shows no comparable effect [$\Delta\delta(\text{C}3=\text{C}4) < 13.4$ only]. In addition, in the case of the *endo*-isomers, long range $\text{C}-\text{H}$ connectivity between H5 and $\text{CN}/\text{CO}-\text{R}$ at the same carbon atom was found from the corresponding HMBC experiments.

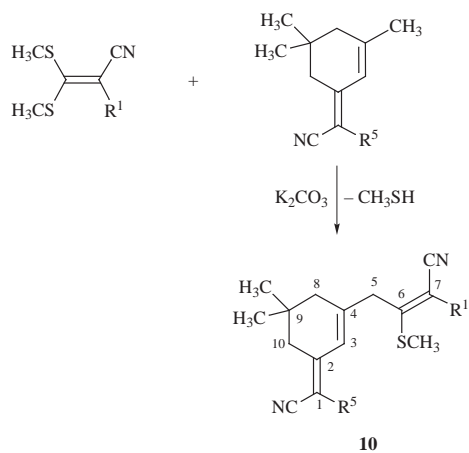
The mass spectrometric fragmentation is also greatly dependent on the *exo/endo*-isomerism of the double bond. Compounds with an *exo* double bond ($\text{R}^5 = \text{CN}$) either do not exhibit the loss of $\text{CH}(\text{CN})_2$ (65 mu) at all (five- and six-membered derivatives) or do so in relatively small amounts (seven- and eight-membered derivatives). All diester derivatives ($\text{R}^1, \text{R}^5 = \text{COOR}'$) and obviously also those derivatives with an ester group on the alkenyl substituent ($\text{R}^5 = \text{CN}, \text{R}^1 = \text{COOR}'$) fragment only or predominantly *via* the *endo* channel, losing the corresponding $\text{CH}(\text{CN})\text{R}^5$ group in agreement with their postulated structures based on the NMR results.

With respect to the *exo/endo*-isomerism of the push-pull alkenes studied, the following major conclusions can be drawn. (i) In the case of the tetracyano compounds **1** only the *exo*-isomers were found and studied by NMR (Tables 1–4); in some of the mass spectra traces of the *endo*-isomer could be identified based on the corresponding $[\text{M} - 65]^+$ peaks.² (ii) With one ester group in the 5-position (**4**, **5**) both isomers could be identified by NMR spectroscopy for the five- and six-membered rings; in the seven- or eight-membered analogues the *endo*-isomers proved to be strongly preferred; however, in the gas phase the *exo*-isomers are still present as concluded from the $[\text{M} - \text{CH}(\text{CN})\text{ester}]^+$ peaks in the EI mass spectra.² (iii) The push-pull olefins with one ester group in the 1-position, **2**, **3** ($\text{R}^5 = \text{CN}, \text{R}^1 = \text{ester}$), and two ester groups in the 1- and 5-positions, respectively, **6–9** ($\text{R}^1 = \text{ester}, \text{R}^5 = \text{ester}$) exist as pure *endo*-isomers both in solution and also in the gas phase.²

E/Z-Isomerism of the $\text{C}1=\text{C}2$ double bond of the push-pull pentadienes **2**, **3**, **6–9**

The push-pull penta-1,3-dienes with one ester group in the 1-position could exist as *E/Z*-isomers with respect to the $\text{C}1=\text{C}2$ double bond; however, the two sets of signals found in both the ^1H and ^{13}C NMR spectra had to be assigned to a rotational kind of stereoisomerism (*vide infra*). In order to assign the prevailing configuration the following arguments were considered.

(i) If the reaction of 3,5,5-trimethylcyclohex-2-en-1-ylidene malonic acid derivatives and the ketene-*S,S*-acetals is studied, the S_{N} reaction takes place (obviously due to steric hindrance) at the allylic methyl group (*cf.* Scheme 3) and not, as usual, at the α -methylene group (*cf.* Scheme 1); accordingly, the push-pull hepta-1,3,6-trienes **10** are obtained. Both the ^1H and ^{13}C NMR spectra of these compounds are given in Tables 5 and 6. The configuration at the push-pull double bond is readily indicated by the ^{13}C chemical shift of the $\text{C}5$ methylene group (being 43.4–43.5 ppm for the *Z*- but 39.4–39.5 ppm for the *E*-configuration). The isomerism was proved also by the X-ray structural analysis of **10** ($\text{R}^1 = \text{COOMe}, \text{R}^5 = \text{CN}$) and **10** ($\text{R}^1 = \text{COOMe}, \text{R}^5 = \text{COOEt}$).¹

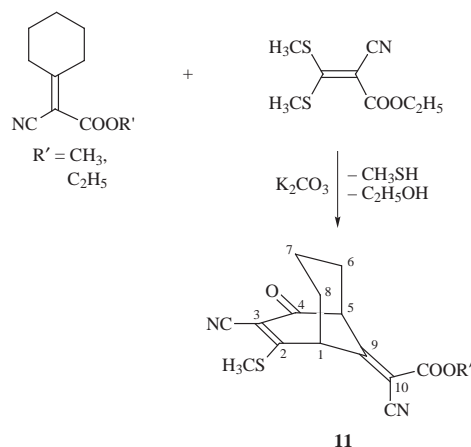


Scheme 3

(ii) The ^{13}C chemical shift of the $\text{S}-\text{Me}$ carbon was at ca. 15 ppm for the *Z*- and at ca. 16 ppm for the *E*-configuration with respect to the ester group (*cf.* Table 6) and was used, accordingly, to assign the configurations present in **2**, **3**, **6–9**; the same ^{13}C chemical shift sequence was found in a number of $(\text{MeS})_2\text{C}=\text{CH}-\text{C}(\text{O})\text{R}$ derivatives.³ Following qualitatively this interpretation, the *E*-configuration at the push-pull C,C double bond in **2**, **3**, **6–9** can also be deduced.

(iii) In order to confirm the configuration at the push-pull C,C double bond, a number of NOE experiments were also carried out by irradiating selectively the $\text{S}-\text{Me}$ protons and *vice versa* if successful. In the homonuclear case only the expected spatial orientation of SMe to $\text{H}5$ was found in the *endo*-isomers; however, in the corresponding heteronuclear experiment, when studying compounds **6–9**, a spatial connectivity of SMe protons to the ester carbonyl carbon of R^5 was proved to exist. Even if only indirect, this information proves qualitatively the spatial distance of SMe to $\text{CO}(\text{R}^1)$ to be larger than that to $\text{CO}(\text{R}^5)$ and, hereby, the *E*-configuration at the push-pull C,C double bond; in the *Z*-configuration a relevant heteronuclear NOE between SMe and $\text{CO}(\text{R}^1)$ can be expected.

(iv) In a few cases of cyclohexylidene malonic esters, the normal push-pull pentadienes were not obtained but instead the intramolecularly cyclized products **11** (Scheme 4); both the



Scheme 4

^1H and ^{13}C NMR spectra of these compounds are given in Tables 7 and 8. We take this result as another experimental proof that the push-pull pentadienes, generated as intermediates in the reaction (Scheme 4), have the *E*-configuration at the push-pull C,C double bond.

(v) The MS study of benzoylketene-*S,S*-acetals⁴ proved that the $[\text{M} - 17]^+$ peak was formed by ejecting the OH radical *via* participation of one $\text{S}-\text{Me}$ proton (proved by $\text{S}-\text{Me}$

Table 4 ^{13}C NMR spectra (δ) of *endo*-isomers **1–9** (solvent CDCl_3 -TMS)

	C1	C2	C3	C4	C5	Remaining ring-C	R ¹	R ⁵	CN	SCH ₃
1 (<i>n</i> = 2, <i>endo</i>)	79.3	179.8	135.8	127.2	40.3	21.3; 25.8; 26.9; 30.2	112.2	109.3	110.2; 111.0	15.9
2 (<i>n</i> = 2, <i>endo</i>)	98.4	176.9	137.8	124.4	30.2	21.4; 26.8; 26.9; 30.2	162.7 (CO) 54.9 (OCH ₃)	110.4	110.6; 114.0	16.0
2 (<i>n</i> = 3, <i>endo</i>)	93.4 95.5 96.6	180.9 181.8 183.3	138.7 140.3 141.0	132.3 133.6 133.7	43.0 45.3 46.0	25.0; 25.3; 25.4; 25.8; 30.5; 31.0; 31.3; 31.7; 34.2; 34.8; 35.0; 35.1	164.3 164.6 164.9 (CO) 52.6 52.8 53.2 (OCH ₃)	118.0	114.5; 114.8 115.4; 115.6	15.6 16.1 16.5
2 (<i>n</i> = 4, <i>endo</i>)	97.3	182.9	139.1	130.5	44.5	24.8; 25.8; 25.9; 29.3; 30.5; 33.7	164.4 (CO) 52.1 (OCH ₃)	114.5	115.4; 116.3	16.5
3 (<i>n</i> = 2, <i>endo</i>)	98.7	177.1	138.1	124.4	27.1	21.5; 21.6; 25.6; 30.3	162.6 (CO) 62.7 (OCH ₂) 14.3 (CH ₃)	110.1	110.9; 114.3	16.2
3 (<i>n</i> = 3, <i>endo</i>)	95.9 96.8 97.0	180.6 181.7 182.8	138.7 140.3 141.1	132.2 133.5 133.6	43.0 45.3 46.0	25.0; 25.3; 25.4; 25.8; 26.0; 30.5; 30.9; 31.0; 31.3; 31.7; 34.8; 35.0; 35.1	164.4 164.6 165.0 (CO) 62.0 62.3 62.7 (OCH ₂) 13.9 14.1 (CH ₃)	118.0	114.1; 114.5; 114.8; 115.4; 115.6	15.6 16.1 16.4
3 (<i>n</i> = 4, <i>endo</i>)	97.7	182.1	140.3	130.6	44.3	24.4; 25.5; 25.9; 29.8; 30.2; 33.1	164.6 (CO) 61.9 (OCH ₂) 14.1 (CH ₃)	114.3	114.8; 116.4	16.1
4 (<i>n</i> = 2, <i>endo</i>)	78.2 79.2	182.0 183.1	133.7 134.4	130.1 130.7	41.9 42.3	21.5; 21.6; 21.7; 25.6; 25.9; 29.9; 30.0	111.8	163.8 164.6 (CO) 54.4 (OCH ₃)	111.5; 111.7 113.5; 114.1	15.7 15.9
4 (<i>n</i> = 3, <i>endo</i>)	77.4 78.2	183.1 184.1	137.9 138.6	136.0 136.4	42.8 43.2	25.2; 25.5; 31.1; 31.8; 34.2	111.2	163.5 164.4 (CO) 54.1 54.2 (OCH ₃)	112.1; 113.7	15.6 16.0
4 (<i>n</i> = 4, <i>endo</i>)	78.1 78.8	182.1 183.4	136.8 137.1	132.9 133.4	41.6 42.7	24.8; 25.3; 28.2; 29.5; 30.0; 32.5	111.2	163.9 164.6 (CO) 53.7 54.2 (OCH ₃)	112.3; 113.3	15.7 16.1
5 (<i>n</i> = 2, <i>endo</i>)	77.3 77.8	182.4 183.5	133.4 133.9	129.4 129.9	42.2 42.3	21.1; 25.3; 25.5; 29.1	111.9 112.0	164.0 164.4 (CO) 62.9 63.2 (OCH ₂) 13.7 13.8 (CH ₃)	112.1; 112.2 114.6; 115.1	15.2 15.4
5 (<i>n</i> = 3, <i>endo</i>)	77.4 78.2	183.2 184.2	137.8 138.5	136.1 136.5	43.1 43.5	25.2; 25.3; 25.5; 25.7; 31.0; 31.1; 31.7; 34.4	112.0	163.0 163.9 (CO) 63.8 (OCH ₂) 13.9 (CH ₃)	111.2; 112.1; 112.9; 113.9	15.7 16.0
5 (<i>n</i> = 4, <i>endo</i>)	78.1 78.7	182.3 183.5	136.8 136.9	133.1 133.5	41.9 43.1	25.3; 26.3; 28.3; 30.0; 32.5; 32.9	111.3	163.5 164.1 (CO) 63.8 63.9 (OCH ₂) 13.9 (CH ₃)	112.2; 112.4 114.1	15.7 16.1
6 (<i>n</i> = 1, <i>endo</i>)	~90	181.7	138.9	132.8	37.5	22.3; 33.6	163.1 (CO) 54.1 (OCH ₃)	162.9 (CO) 52.7 (OCH ₃)	113.1; 114.5	15.9
6 (<i>n</i> = 3, <i>endo</i>)	96.9 97.6	180.5 181.1	139.5 140.4	123.9 133.2	42.8 43.1	24.9; 25.5; 31.2; 31.9; 34.7	163.1 (CO) 53.8 53.9 (OCH ₃)	163.8 164.7 (CO) 52.6 52.7 (OCH ₃)	113.2; 114.1 115.2; 115.4	15.9 16.3
6 (<i>n</i> = 4, <i>endo</i>)	97.6 98.0	180.0 180.5	138.5 138.7	130.2 130.4	41.5 42.8	24.6; 25.2; 28.1; 29.6; 30.0; 33.3	164.4 164.9 (CO) 53.5 53.9 (OCH ₃)	163.1 163.2 (CO) 52.7 52.8 (OCH ₃)	113.6; 114.2 115.4; 115.7	16.0 16.2
7 (<i>n</i> = 1, <i>endo</i>)	~90	181.7	138.8	132.5	37.5	22.3; 32.3; 37.7	163.1 (CO) 52.7 (OCH ₃)	162.9 (CO) 63.7 (OCH ₂) 13.8 (CH ₃)	112.0; 114.5	15.9
7 (<i>n</i> = 3, <i>endo</i>)	97.4 98.8	180.0 180.3	138.3 138.4	131.2 131.8	41.9 43.0	24.7; 26.4; 29.5; 33.3; 33.8	164.9 165.2 (CO) 50.1 51.2 (OCH ₃)	163.4 163.6 (CO) 62.9 (OCH ₂) 13.5 (CH ₃)	113.9; 114.2 115.3; 115.7	15.3
7 (<i>n</i> = 4, <i>endo</i>)	97.9 98.0	180.1 180.5	138.5 138.7	130.2 130.5	41.7 43.0	24.7; 26.4; 28.1; 29.5; 33.3; 33.8	163.9 164.4 (CO) 52.7 52.8 (OCH ₃)	163.1 163.2 (CO) 63.5 (OCH ₂) 13.9 (CH ₃)	113.7; 114.4 115.5; 115.7	16.1
8 (<i>n</i> = 1, <i>endo</i>)	~90	182.0	138.3	132.2	37.5	22.3; 33.6	163.6 (CO) 62.1 (OCH ₂) 14.0 (CH ₃)	162.5 (CO) 52.8 (OCH ₃)	113.2; 114.5	15.9

Table 4 (cont)

	C1	C2	C3	C4	C5	Remaining ring-C	R ¹	R ⁵	CN	SCH ₃
8 (<i>n</i> = 3, <i>endo</i>)	97.3	180.0	139.6	132.8	42.8	25.0; 25.5; 30.7; 31.7;	162.7	163.9	113.3; 114.1	15.9
	98.1	180.7	140.5	133.1	43.1	34.8	162.8 (CO) 62.1 (OCH ₂) 14.1 (CH ₃)	164.7 (CO) 53.8 53.9 (OCH ₃)	115.2; 115.3	16.3
8 (<i>n</i> = 4, <i>endo</i>)	98.0	179.5	138.6	130.1	41.5	25.0; 25.5; 30.7; 31.7;	162.7	163.9	113.1; 114.1	15.9
	98.5	180.0	138.9	130.3	42.8	34.8	162.8 (CO) 62.1 (OCH ₂) 14.1 (CH ₃)	164.7 (CO) 53.8 53.9 (OCH ₃)	115.2; 115.3	16.3
9 (<i>n</i> = 1, <i>endo</i>)	93.4	182.8	138.9	132.4	37.4	22.4; 37.8	163.1 (CO) 63.7 (OCH ₂) 14.1 (CH ₃)	162.5 (CO) 63.4 (OCH ₂) 13.8 (CH ₃)	112.0; 114.6	15.8
9 (<i>n</i> = 3, <i>endo</i>)	98.4	180.2	138.6	132.4	42.1	24.8; 25.3; 31.1; 33.6;	161.1	163.2	113.6; 114.4	16.1
	98.9	180.7	139.1	133.1	43.2	34.6	162.9 (CO) 64.9 (OCH ₂) 13.6 (CH ₃)	164.8 (CO) 63.5 (OCH ₂) 13.6 (CH ₃)	115.3; 115.6	
9 (<i>n</i> = 4, <i>endo</i>)	97.3	180.4	139.6	132.9	43.0	24.9; 25.3; 30.6; 31.3;	162.7	163.4	113.3; 114.2	16.3
	98.0	180.7	140.3	133.2	43.3	34.7; 34.9	162.8 (CO) 63.5 (OCH ₂) 13.9 (CH ₃)	164.2 (CO) 62.0 (OCH ₂) 13.8 (CH ₃)	115.2; 115.4	

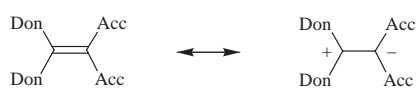
Table 5 ¹H NMR spectra (δ) of compounds **10** (solvent CDCl₃-TMS)

10 (R ¹ , R ⁵)	H3	H5	Remaining ring-H	Ring-CH ₃	R ¹	R ⁵	SCH ₃
(CN, CN)	6.71 (s, 1H)	3.72 (s, 2H)	2.22 (s, 2H); 2.61 (s, 2H)	1.06 (s, 6H)			2.68 (s, 3H)
(COOMe, CN)	6.62 (s, 1H)	3.83 (s, 2H)	2.27 (s, 2H); 2.59 (s, 2H)	1.05 (s, 6H)	3.87 (s, 3H)		2.42 (s, 3H)
(COOEt, CN)	6.57 (s, 1H)	3.86 (s, 2H)	2.25 (s, 2H); 2.57 (s, 2H)	1.04 (s, 6H)	4.24 (q, 2H) 1.34 (t, 3H)		2.42 (s, 3H)
	6.63 (s, 1H)	4.13 (s, 2H)	2.27 (s, 2H); 2.60 (s, 2H)	1.06 (s, 6H)	4.29 (q, 2H) 1.37 (t, 3H)		2.54 (s, 3H)
(COOMe, COOMe)	6.71 (s, 1H)	3.79 (s, 2H)	2.19 (s, 2H); 2.58 (s, 2H)	1.01 (s, 6H)	3.87 (s, 3H)	3.83 (s, 3H)	2.45 (s, 3H)
(COOEt, COOMe)	7.60 (s, 1H)	4.20 (s, 2H)	2.19 (s, 2H); 2.60 (s, 2H)	1.03 (s, 6H)	4.30 (q, 2H) 1.32 (t, 3H)	3.83 (s, 3H)	2.54 (s, 3H)
(COOMe, COOEt)	7.57 (s, 1H)	4.09 (s, 2H)	2.20 (s, 2H); 2.58 (s, 2H)	1.03 (s, 6H)	3.81 (s, 3H)	4.29 (q, 2H) 1.35 (t, 3H)	2.54 (s, 3H)
(COOEt, COOEt)	7.58 (s, 1H)	4.09 (s, 2H)	2.19 (s, 2H); 2.58 (s, 2H)	1.02 (s, 6H)	4.29 (q, 2H) 1.35 (t, 3H)	4.24 (q, 2H) 1.32 (t, 3H)	2.53 (s, 3H)

deuteration); this kind of fragmentation could not be expected in the *E*-configuration (obviously present) and hence the corresponding fragmentation is completely missing from **2**, **3**, **6–9** but has been observed in **10** (R¹ = COOMe, R⁵ = CN) and **10** (R¹ = COOMe, R⁵ = COOEt) which were found also in the *Z*-configuration.

Push-pull character of 1–11

The studied compounds consist of one or two push-pull C,C double bonds (both C1–C2 and C4–C5 in the *exo*-isomers of **1–9** but only C1–C2 in the *endo*-analogues; so also two, in both **10** and in **11**). As a useful measure to quantify the push-pull effect the degree of π -polarization (charge separation—*cf.* Scheme 5),



Scheme 5

the barrier to rotation about the central C,C double bond (ΔG^\ddagger) and the ¹³C chemical shift difference of the two olefinic carbon atoms ($\Delta\delta_{C,C}$) were employed.³ No barrier to rotation about the corresponding partial C,C double bonds could be found; obviously, the presence of only two acceptor substituents and/or two acceptor substituents/one donor substituent is insufficient to reduce the double bond character enough to lower the rotational barrier sufficiently as to allow fast rotation on the NMR timescale. This is in line with the previous results for RR'C=CR''R''' (see Table 9).

Even if a second donor substituent SMe is present, the expected barrier to rotation is still too high to be experimentally

measured ($\Delta G^\ddagger > 100 \text{ kJ mol}^{-1}$). The second parameter, the ¹³C chemical shift difference of the two olefinic carbon atoms ($\Delta\delta_{C,C}$), looks more promising. However, it is not a quantitative measure of the push-pull effect but only a fingerprint of the π -polarization of the partial push-pull C,C double bond by the present donor/acceptor combination. Within this context, the push-pull parameter $\Delta\delta_{C,C}$ can be discussed as follows.

(i) The push-pull character of the C1,C2 and C4,C5 partial double bonds in the *exo*-isomers of **1–9**, only that of C1,C2 in the *endo*-analogues and both of the corresponding two bonds in **10** and **11** are remarkably indicated by the chemical shift difference of the two relevant carbon atoms $\Delta\delta_{C1,C2}$, *e.g.* **5** (*n* = 3, *endo*) $\Delta\delta_{C1,C2} = 104.2$ and 104.8 (for the two rotamers; see below); **5** (*n* = 1, *exo*) $\Delta\delta_{C1,C2} = 106.9$; $\Delta\delta_{C4,C5} = 74.6$ (for the two rotamers; see below).

(ii) In the latter example the quantitative nature of this parameter is remarkably corroborated; the additional donor substituent SMe at C2 increases the push-pull character, indicated by the larger π -electron polarization, by 32.3 ppm.

(iii) Also the larger acceptor power of CN with respect to COOR'⁸ is generally and correctly reproduced, *e.g.* **4** (*n* = 3, *endo*) $\Delta\delta_{C1,C2} = 105.7$ and 105.9 , but **6** (*n* = 3, *endo*) $\Delta\delta_{C1,C2} = 83.5$ and 83.6 (for the two rotamers; see below).

(iv) Within this context, the methyl ester proved to be the stronger acceptor substituent compared with the corresponding ethyl ester analogue [*cf.* *e.g.* **6** (*n* = 3, *endo*) and **7** (*n* = 3, *endo*)].

Conformation and stereodynamics of the push-pull pentadienes 1–9

NMR spectra. In the NMR spectra of the six-, seven- and eight-membered ring push-pull pentadienes **1–9** at room temperature two sets of signals of different intensity were obtained.

Table 6 ^{13}C NMR spectra (δ) of compounds **10** (solvent CDCl_3 -TMS)

10 (R^1, R^5)	C1	C2	C3	C4	C5	C6	C7	Remaining ring-C	Ring- CH_3	R^1	R^5	CN	SCH_3
(CN, CN)	152.6	122.2	168.2	82.1	43.5	178.2	80.7	43.0; 32.3; 42.4	27.6	111.5	111.3	112.1; 112.2	16.1
(COOMe, CN)	154.2	120.7	168.5	81.5	43.5	175.3	100.2	43.4; 32.3; 42.6	27.6	162.8 (CO) 52.7 (OCH_3)	111.5	112.4; 115.4	15.8
(COOEt, CN)	156.3	120.0	169.0	80.5	39.5	175.1	100.4	43.6; 32.3; 42.6	27.6	160.9 (CO) 62.0 (OCH_2) 13.9 (CH_3)	111.7	112.6; 114.5	15.1
	154.4	120.6	168.5	81.4	43.4	174.9	100.7	43.6; 32.3; 42.6	27.6	160.9 (CO) 62.2 (OCH_2) 14.0 (CH_3)	111.5	112.4; 115.5	15.8
(COOMe, COOMe)	151.7	120.4	164.5	101.5	39.5	176.2	100.0	43.6; 32.3; 42.8	27.8	162.9 (CO) 52.7 (OCH_3)	162.8 (CO) 52.5 (OCH_3)	115.3; 115.6	15.7
(COOEt, COOMe)	152.3	120.3	164.5	100.1	39.5	176.8	99.9	43.6; 32.3; 43.6	27.8	164.4 (CO) 61.9 (OCH_2) 14.1 (CH_3)	162.3 (CO) 52.5 (OCH_3)	114.8; 116.4	14.9
(COOMe, COOEt)	152.3	120.3	164.0	100.7	39.4	177.5	99.2	43.6; 32.2; 44.2	27.7	161.4 (CO) 52.6 (OCH_3)	161.9 (CO) 61.7 (OCH_2) 14.1 (CH_3)	114.8; 116.8	14.9
(COOEt, COOEt)	152.4	120.4	164.0	100.7	39.4	176.9	99.7	43.6; 32.2; 44.2	27.7	160.9 (CO) 61.7 (OCH_2) 14.0 (CH_3)	161.9 (CO) 61.8 (OCH_2) 14.1 (CH_3)	114.8; 116.4	14.8

Table 7 ^1H NMR spectra (δ) of compounds **11** (solvent CDCl_3 -TMS)

	H1	H5	Remaining ring-H	COOR'	SCH ₃
11 ($\text{R}' = \text{CH}_3$)	5.75 (m, 1H)	3.95 (m, 1H)	1.92; 2.31 (m, 2H) 1.66; 1.77 (m, 2H) 2.01; 2.06 (m, 2H)	3.89 (s, 3H)	2.73 (s, 3H)
11 ($\text{R}' = \text{C}_2\text{H}_5$)	5.76 (m, 1H)	3.96 (m, 1H)	1.91; 2.30 (m, 2H) 1.64; 1.71 (m, 2H) 2.03 (m, 2H)	4.32 (q, 2H) 1.38 (t, 3H)	2.72 (s, 3H)

Table 8 ^{13}C NMR spectra (δ) of compounds **11** (solvent CDCl_3 -TMS)

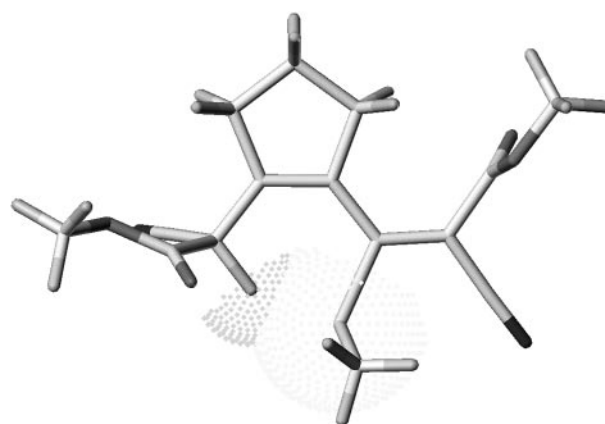
	C1	C2	C3	C4	C5	C9	C10	Remaining ring-C	COOR'	CN	SCH ₃
11 ($\text{R}' = \text{CH}_3$)	39.4	178.1	110.2	187.5	53.2	172.2	102.1	17.0; 31.8; 33.5	161.6 (CO) 53.3 (OCH ₃)	112.2; 113.2	16.1
11 ($\text{R}' = \text{C}_2\text{H}_5$)	39.2	178.3	110.1	187.6	53.6	171.7	102.5	16.9; 31.7; 33.4	161.1 (CO) 62.8 (OCH ₂) 13.9 (CH ₃)	112.2; 113.2	15.2

Table 9 Barrier to rotation about $\text{C}=\text{C}$ double bond (ΔG^\ddagger) for compounds $\text{RR}'\text{C}=\text{CR}''\text{R}'''$

R	R'	R''	R'''	$\Delta G^\ddagger/\text{kJ mol}^{-1}$	Ref.
SMe	SMe	OCOMe	CN	103	5
SMe	SMe	COMe	COOMe	>105	5
SMe	Me	COOMe	COOMe	>115	6
-CH=C(Me)-O-C(Me)=CH-		COOMe	CN	>113	7
-CH=C(Me)-S-C(Me)=CH-		COOMe	CN	>113	7
SMe	SMe	SPh	CN	>100	8
SMe	SMe	SPh	COOMe	>100	8
SMe	SMe	S(O)Ph	CN	>100	8
SMe	SMe	S(O)Ph	COOMe	>100	8
SMe	SMe	H	C(O)Ph	>100	3

Immediately after the solution was prepared, only one stereoisomer (the major one) was observed from the NMR spectrum; after a short time the signals of the second stereoisomer were also generated and finally reached a constant ratio to the other form at a certain temperature. If the temperature is increased, the ratio of the two stereoisomers further alters to the disadvantage of the major isomer. In the case of the five-membered ring analogues the same effect was found but below ambient temperature. *E/Z*-Isomerism at the C1,C2 push-pull double bond has already been excluded as being the reason for the stereoisomerism observed (*vide supra*). The fact that this isomerism was also found for the compounds with $\text{R}^1 = \text{CN}$, $\text{R}^5 = \text{COOR}'$ is another and independent proof for this interpretation. On raising the temperature above the coalescence temperature (T_c) the signal sets broaden, collapse into the base line and sharpen into common signals. Restricted rotation about the C2-C3 single bond is the only viable explanation for the dynamic phenomena. These dynamic exchange effects were observable on more or less all signals both in the ^1H and ^{13}C NMR spectra although a signal overlap very often restricted detailed analysis; only S-Me, H5 or H3 and the ester alkyl signals could be studied in detail and were employed for extracting the barriers to rotation (*cf.* Table 10). The free energies of activation ΔG^\ddagger were calculated at the coalescence temperature T_c by the method of Shanan-Atidi and Bar-Eli⁹ which is described in detail in ref. 10. Both the chemical shift differences $\Delta\nu(\text{Hz})$ and the population differences (ΔP) of the participating stereoisomers were extrapolated to $T_c(\text{K})$. The following conclusions could be drawn from the barriers to rotation obtained (*cf.* Table 10).

(i) In the series of five-membered rings ($n = 1$) the steric barrier proved to be lower in the compounds with the *exo*-double bond compared with the *endo* analogues (*exo*: $\text{R}^5 = \text{ester}$, $\text{R}^1 = \text{CN}$, $\Delta G^\ddagger = 47\text{--}49.6 \text{ kJ mol}^{-1}$ but *endo*: $\text{R}^5 = \text{ester}$, $\text{R}^1 = \text{ester}$, $\Delta G^\ddagger = 59.2\text{--}62.7 \text{ kJ mol}^{-1}$). The reason for this effect is sp^2 hybridisation of C5 in the *exo*-isomers; H5 in the *endo* analogues sterically hinders the transition state of the restricted

**Fig. 1** Structure of the transition state (TS) of the restricted rotation about the C2-C3 single bond in **6** ($n = 1$, *endo*) showing the sterically destabilizing $\text{H5} \cdots \text{SMe}$ interaction

rotation. In this transition state the whole C3 substituent is forced to be more or less planar with the ring system and the C4 substituent must be perpendicular to it, H5 thus sterically hindering the latter conformation and destabilizing the transition state of the dynamic process (*cf.* Fig. 1).

(ii) The barriers to rotation for the *endo*-isomers of the six-, seven- and eight-membered push-pull pentadienes are larger (barriers of the *exo*-analogues could not be measured). Obviously the spatial situation in the five-membered ring systems for the conformational stabilization of the transition state of the restricted rotation is much better due to bond angle advantages. In the larger ring systems the two adjacent C3- and C4-substituents are closer together; hereby the transition state will be more destabilized and, accordingly, the barrier to rotation substantially raised.

(iii) If the same dynamic process is studied in a less polar

Table 10 Dynamic NMR data for the *exolendo*-isomeric push-pull pentadienes 1–9

No.	Configuration	Solvent	Ring size, <i>n</i>	Signal studied	R ¹	R ⁵	R ^{Ring}	<i>T</i> _c /K	<i>k</i> /Hz	Δ <i>G</i> [‡] /kJ mol ⁻¹
2	<i>exo</i>	CD ₂ Cl ₂	1	SMe	COOMe	CN	—	226	19	49.3
									65	47.0
3	<i>exo</i>	CD ₂ Cl ₂	1	SMe	COOEt	CN	—	227	18	49.6
									64	47.2
6	<i>endo</i>	CD ₂ Cl ₂	1	SMe	COOMe	COOMe	—	283	18/42	62.4/60.4
7	<i>endo</i>	CD ₂ Cl ₂	1	SMe	COOMe	COOEt	—	278	16/44	61.5/59.2
8	<i>endo</i>	CD ₂ Cl ₂	1	SMe	COOEt	COOMe	—	285	19/43	62.7/60.8
9	<i>endo</i>	CD ₂ Cl ₂	1	SMe	COOEt	COOEt	—	281	19/44	61.8/59.8
2	<i>endo</i>	[² H ₇]DMF	2	H1	COOMe	CN	—	373	20/33	82.9/81.4
		[² H ₇]DMF		OMe				363	11/19	82.3/80.6
		[² H ₇]DMF		SMe				367	12/20	83.0/81.4
		[² H ₂]TCE		H1				345		77.4
		[² H ₂]TCE		SMe				355		78.8
3	<i>endo</i>	[² H ₇]DMF	2	H1	COOEt	CN	—	375	25/31	82.6/81.9
		[² H ₇]DMF		SMe				368	18/24	81.9/81.1
2	<i>endo</i>	[² H ₇]DMF	2	H1	COOMe	CN	5'-Me	368	15/31	82.5/80.2
4	<i>endo</i>	[² H ₇]DMF	2	H1	CN	COOEt	—	375	41/51	81.0/80.3
5	<i>endo</i>	[² H ₇]DMF	2	H1	CN	COOMe	—	383	26/57	84.2/81.7
				OMe				383	12/25	86.8/84.3
2	<i>endo</i>	[² H ₇]DMF	3	H1	COOMe	CN	—	390	17/35	87.2/84.8
3	<i>endo</i>	[² H ₇]DMF	3	H1	COOEt	CN	—	393	39/39	85.2/85.2
6	<i>endo</i>	[² H ₆]Acetone	3	H1/SMe	COOMe	COOMe	—	>330	—	—
	<i>endo</i>	[² H ₂]TCE	3	H1/SMe	COOMe	COOMe	—	>420	—	—
4	<i>endo</i>	[² H ₂]TCE	3	H1/SMe	CN	COOMe	—	>420	—	—
2	<i>endo</i>	[² H ₇]DMF	4	H1	COOMe	CN	—	382	32/37	83.3/82.9
3	<i>endo</i>	[² H ₇]DMF	4	H1	COOEt	CN	—	365	28/33	80.0/79.4
		[² H ₂]TCE		H1				320		77.3/76.2
4	<i>endo</i>	[² H ₂]TCE	4	H1	CN	COOMe	—	>420	—	—
6	<i>endo</i>	[² H ₂]TCE	4	H1	COOMe	COOMe	—	>420	—	—

solvent (1,1,2,2-tetrachloroethane–[²H₂]TCE) the barrier to rotation is reduced by 3–5 kJ mol⁻¹; hence this solvent is unable to stabilize the ground state conformers. The latter influence is diminished in the corresponding transition states; here the in-plane position of the C3 substituent prevents solvent stabilization in this kind of conformation.

(iv) It was impossible to determine the barrier to rotation about the C²–C³ single bond in the *endo*-isomers of the six-, seven- and eight-membered push-pull pentadienes with one ester substituent at the push-pull C1=C2 double bond [except for 2, 3 (*n* = 2, *exo*)].¹¹ With the slightest trace of an acidic/basic impurity in the solution or corresponding properties of the employed solvent, the compounds decompose; only 1,1,2,2-tetrachloroethane could be used where the decomposition processes are slower but this evaporates at *ca.* 150 °C. Both the lower acceptor power of the COOR' substituents compared with CN and extended steric hindrance due to the more voluminous COOR' with respect to CN can further decrease the stability of the transition state of the dynamic process in question and, hereby, increase the barrier to rotation so much that it could not be reached under the available conditions. This topic will be discussed again when dealing with the results of the *ab initio* quantum chemical calculations.

(v) Barriers to rotation in benzyldenemalononitrile derivatives have been already measured previously.¹² However, the lack of both the bulky thiomethyl substituent and another malononitrile substituent in the 4-position decreases dramatically the corresponding barrier to rotation; the Δ*G*[‡] values were reported to be in the range of 31–41 kJ mol⁻¹.¹²

Quantum chemical calculations. The stereodynamics of the push-pull pentadienes 1–9 were also studied by semi-empirical quantum chemical calculations employing the PM3 method. The mechanism of the dynamic process revealed by the dynamic NMR spectroscopy was thus shown to be a sterically restricted rotation about the C2–C3 single bond; in the following, the results will be discussed for the five-membered ring system as an example. In principle, the same results have been obtained for some of the larger ring analogues.

The calculations gave for the *exo*-isomer 6 (*n* = 1, *exo*) two

ground state conformations with torsional angles S–C2–C3–C4 of –143.7° (–Δ*rH* = 257.9 kJ mol⁻¹) and 44.4° (258.6 kJ mol⁻¹). In these conformations the C3-substituent is more or less perpendicular to the five-membered ring system, thus minimizing the steric hindrance, in particular with the C4-substituent (Fig. 2). The two conformations have roughly the same stability (Δ*H*^o = 0.7 kJ mol⁻¹) as found already from the NMR spectra when the restricted rotation was slow on the NMR timescale (Table 10). If the orientation of the C3-substituent deviates from these most stable dihedral angles, the energy of the molecule increases up to the transition states at torsional angles of –55.7° (–Δ*rH* = 219.0 kJ mol⁻¹) and 114.6° (216.0 kJ mol⁻¹), respectively (*cf.* Fig. 2); here the C3-substituent is more in plane with the five-membered ring system and van der Waals overlap of the C3-substituent and the protons of the five-membered ring in particular destabilize these transition state conformations and accordingly hinder the rotation about the C2–C3 single bond. The energy difference between the two sets of conformations, the barrier to rotation –Δ*H*[‡] = 38.9 and 42.6 kJ mol⁻¹, is in satisfactory agreement with the free energy barrier determined by NMR spectroscopy (*cf.* Table 10); further barriers to rotation, also calculated, are markedly smaller than those studied by dynamic NMR spectroscopy. The stereodynamics and the conformations involved are somewhat different for the *endo*-isomers, *e.g.* for the *endo*-analogue 6 (*n* = 1, *endo*). The two ground state conformations have similar dihedral angles S–C2–C3–C4 of –98.9° (–Δ*rH* = 280 kJ mol⁻¹) and 94.7° (275.9 kJ mol⁻¹) both having the C3 substituent perpendicular to the plane of the five-membered ring system again to minimize the steric interactions (*cf.* Fig. 3). However, the rotation of the C3 substituent can occur only toward smaller dihedral angles—only the S-methyl is able to pass H5 of the C4-substituent (transition state at –0.7° and –Δ*rH* = 239.9 kJ mol⁻¹). The other side of the C3 substituent, in this case Cl(CN)COOMe, is unable to pass this position by rotation. Thus, the dynamic process studied in dynamic NMR spectroscopy in the case of the *endo*-isomers proved to be only a rocking of the C3-substituent about the C2–C3 single bond between dihedral angles S–C2–C3–C4 of *ca.* –100° and *ca.* 95°.

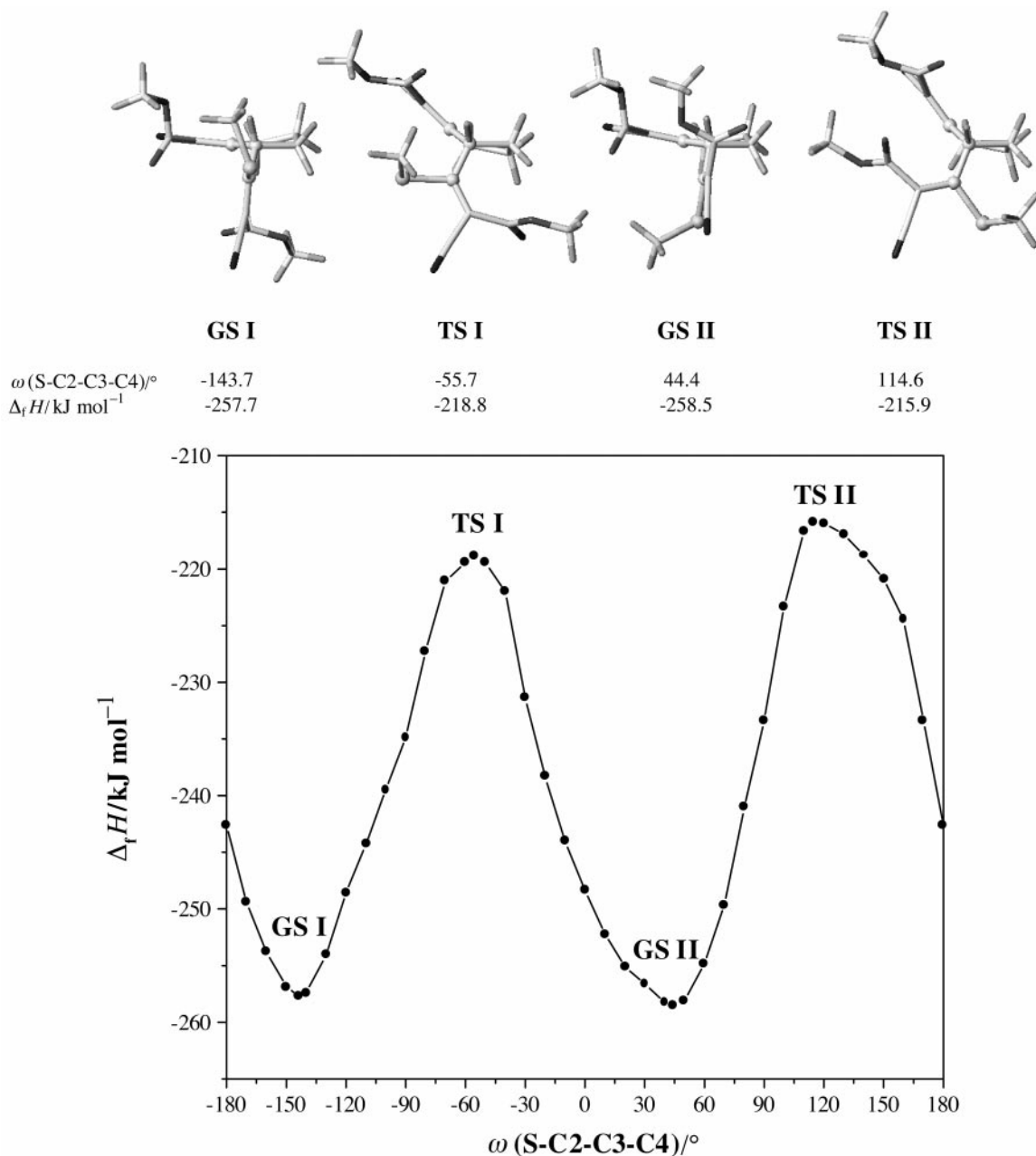


Fig. 2 PM3 calculation of changes in the total energy with the dihedral angle between S–C2–C3–C4 of **6** ($n = 1$, *exo*). The reaction coordinate employed a constrained rotation of the torsion in 10° angle increments. At each step, the remaining degrees of freedom were optimized to obtain the fully minimized structures.

The barrier to rotation was calculated to be $\Delta H^\ddagger = 35.9$ and 40.1 kJ mol^{-1} and hence $\Delta H^\circ = 4.2 \text{ kJ mol}^{-1}$ in good agreement with the experimental findings.

The last result especially prompted us to repeat the stereodynamic calculations at the level of *ab initio* quantum chemistry. The compounds proved flexible not only around the C2–C3 bond but also around all other bonds and the ring systems included had to be energetically optimized to find the ground state/transition state conformations. This procedure was extremely time-consuming; even using our brand new Silicon Graphics Origin 2000 with 14 processors it took several weeks for one compound. However, this expense proved to be very profitable.

The five-membered push-pull pentadienes **6** ($n = 1$) were completely subjected to this procedure at the MO *ab initio* HF/3-21G level; the ground state conformers were calculated to be structurally similar to those obtained from the semi-empirical calculations [*cf.* Fig. 4 for **6** ($n = 1$, *endo*)]. The C3-substituent is positioned perpendicular to the rest of the molecule (torsional angles S–C2–C3–C4 = -90° and 96.4°), in the transition state it

is forced nearly in-plane (torsional angle S–C2–C3–C4 = 36.7° , *cf.* Fig. 4). Both the energy difference between the two ground state conformers ($\Delta E^\circ = 7.16 \text{ kJ mol}^{-1}$) and the energy of activation (barrier to rotation $\Delta E = 61.0 \text{ kJ mol}^{-1}$) are in excellent agreement with the corresponding experimental results (*cf.* Table 10). Thus, the *ab initio* calculations strongly corroborate both the dynamic process present and the ground state conformers revealed by dynamic NMR spectroscopy.

The energetic optimization of the stereochemistry of **6** ($n = 1$) was also carried out with the *Z*-isomers at the C1,C2 push-pull double bond; the corresponding structures were found to be at least 5.28 kJ mol^{-1} less stable than the corresponding *E*-structures. Also in this case the experimental NMR spectroscopic results were markedly supported.

Conclusions

The studied push-pull pentadienes **1–9** were proved to exist as *exolendo*-isomers with respect to the C1,C2 push-pull double bond. Both this isomerism and configuration at the push-pull

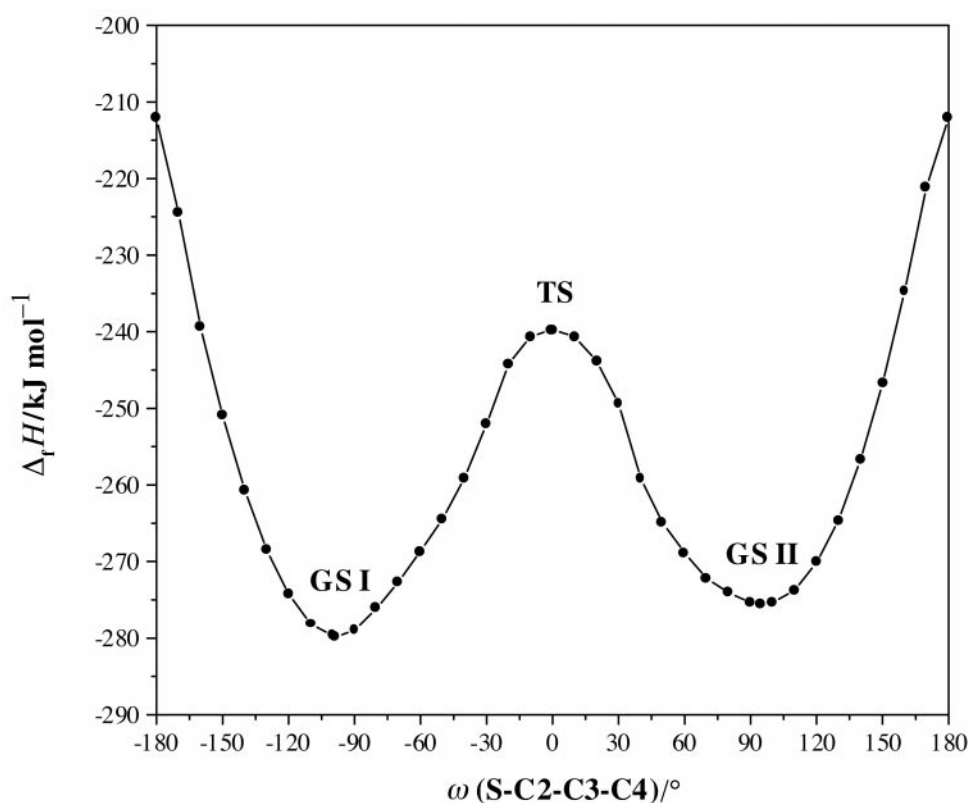
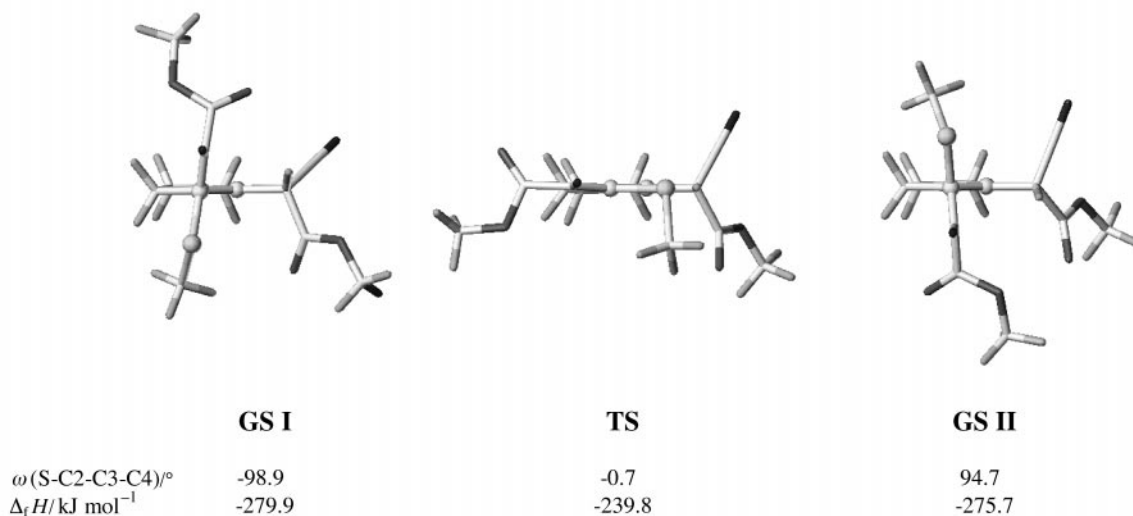


Fig. 3 PM3 calculation of changes in the total energy with the dihedral angle between S-C2-C3-C4 of **6** ($n = 1$, *endo*). The reaction coordinate employed a constrained rotation of the torsion in 10° angle increments. At each step, the remaining degrees of freedom were optimized to obtain the fully minimized structures.

C1,C2 double bond (which is generally *E* in the case of $R^1 \neq \text{CN}$) was assigned by the combined use of NMR and MS. The push-pull character of the C1,C2 bond was proved too low to reduce the bond order enough to make the corresponding barrier to rotation measurable; however, the two stereoisomers, generally found, could be assigned to the ground state conformers of **1-9** which have the C3 substituent perpendicular to the plane of the ring system; the related dynamic process was identified to be the sterically restricted rotation about the C2-C3 bond. Both the standard Gibbs energy differences (ΔG°) between the two conformers and the barriers to rotation (ΔG^\ddagger) being both solvent and temperature dependent were determined by the methodology of dynamic NMR spectroscopy. Semi-empirical (PM3) and *ab initio* (HF/3-21G level) quantum chemical calculations were employed to illustrate the stereo-

dynamics of **1-9** and the results thus obtained were completely in line with the experimental results.

Experimental

NMR spectroscopy

The NMR spectra were obtained using an ARX 300 (Bruker). All samples were dissolved in CDCl_3 or, in the case of low-temperature measurements, in CD_2Cl_2 . High-temperature measurements were carried out using $[\text{}^2\text{H}_7]\text{DMF}$ and $[\text{}^2\text{H}_2]\text{-1,1,2,2-tetrachloroethane}$ as solvent. The 2D spectra were acquired using the standard Bruker software. Typical parameters were for (i) COSY-45: spectral width 2620 Hz, 1k data points in F_2 , 128 experiments in F_1 (16 scans, four dummy scans), relaxation delay 1 s; (ii) HMQC: spectral width in F_2 12

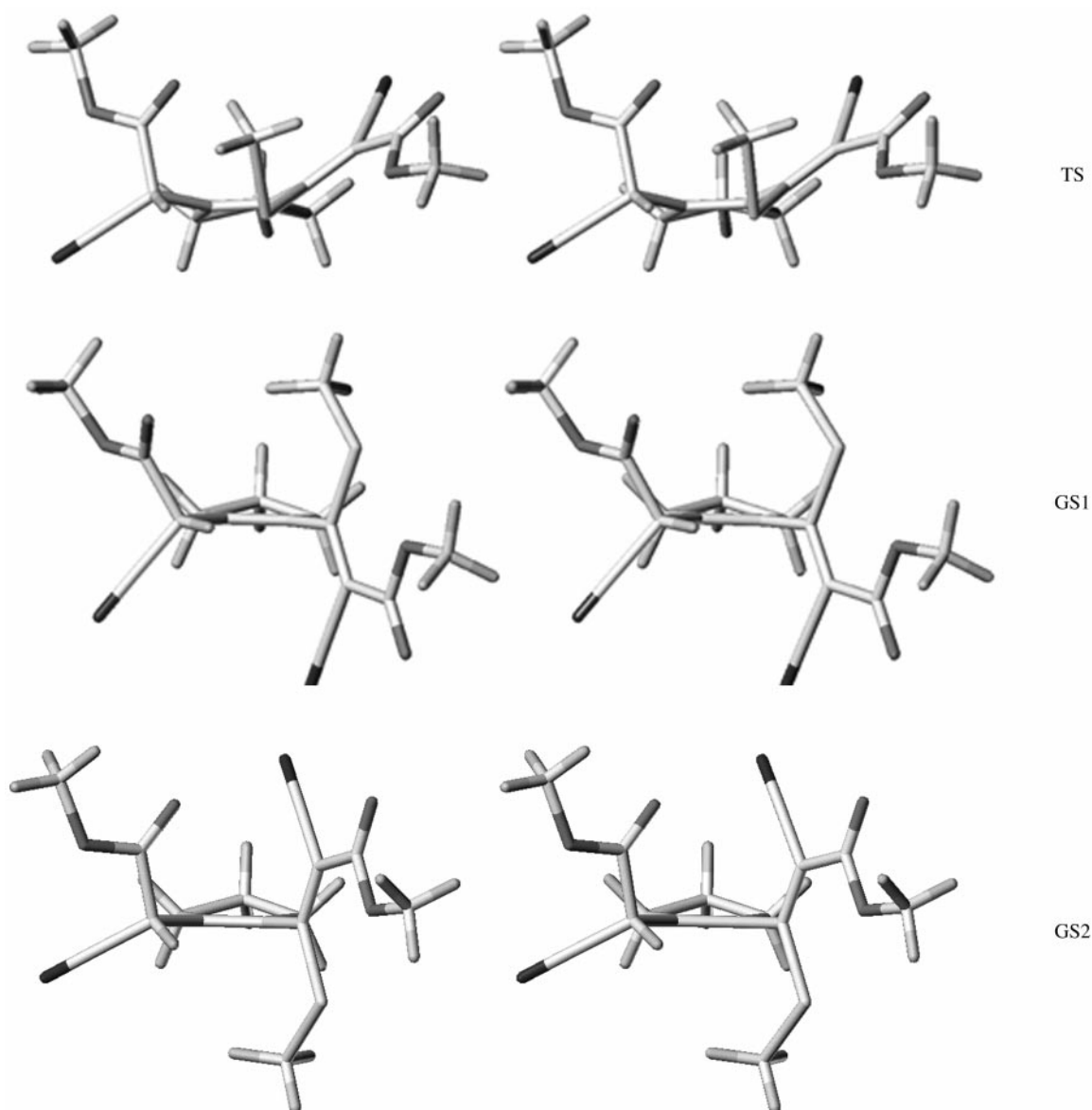


Fig. 4 Chemical structure of the two ground states and the transition state of **6** ($n = 1$, *endo*) during the sterically restricted rotation about the C2–C3 single bond as obtained by quantum chemical *ab initio* calculations (HF/3-21G level)

kHz and in F_2 2620 Hz, 1k data points in F_2 , 128 experiments in F_1 (32 scans, four dummy scans), relaxation delay 1.2 s, delay for inversion recovery 340 ms, zero filling, 1k data points in F_2 and 256 data points in F_1 , filter function shifted square sine-bell in both dimensions; (iii) HMBC: spectral width in F_1 15 kHz and in F_2 2620 Hz, 1k data points in F_2 , 128 experiments in F_1 (128 scans, four dummy scans), relaxation delay 1.2 s, delay for evolution of long-range couplings 55 ms, zero filling, 1k data points in F_2 and 256 data points in F_1 , filter function shifted square sine-bell in both dimensions. The pulse widths (90°) for all experiments were 12.5 μs (^1H), and 11.3 μs (^{13}C), respectively.

Theoretical methods

The semi-empirical calculations were carried out with the program MOPAC 7.0 using the PM3-hamiltonian.¹³ The molecular modelling software package SYBYL 6.4¹⁴ served as a facility to build up and edit starting geometries and visualize the results. Geometry optimization within SYBYL 6.4 (to obtain pre-optimized geometries for the MOPAC minimizations) was carried out using the TRIPOS force field; within MOPAC 7.0 the eigenvector following (EF) method¹⁵ was used. The dynamic process stated above depends not only on the rotation about the C2–C3 single bond but also on the rotation about the single bonds C2–S and C4–C5 (in the case of an endocyclic com-

pound), respectively. Thus, after energy minimization of the starting geometries the torsional angles about the latter bonds were varied stepwise while keeping the torsional angle about the bond C2–C3 at its minimum value and optimizing the remaining internal coordinates to obtain the most stable orientations about these bonds. Using the predetermined geometries, the barrier to rotation about the C2–C3 single bond was calculated by a stepwise variation of the torsional angle S–C2–C3–C4 in 10° increments while fully optimizing all other geometry parameters. Finally, the stationary points of the resulting potential energy surface for the rotation about the C2–C3 bond were further optimized to achieve the ground and transition state conformations.

The *ab initio* calculations were carried out using the program GAUSSIAN94¹⁶ at the HF/3-21G¹⁷ level of theory. All conformations were fully optimized at this level.

The determination of the transition state of the studied dynamic process proved difficult. The use of the QST algorithms¹⁸ does not help because of a multiple variation of several torsional angles during the rotational process: the torsion angles into the five-membered ring system, the torsion angle of the substituent in the 4-position and, additionally, the torsion angles about the bonds C1–R¹ and C5–R⁵. Therefore, in the first step all rotational barriers around these torsion angles

were calculated to find out the flexible areas of every rotation. Then, the rotational barrier about the C2–C3 bond were determined by a stepwise variation of the corresponding torsion angle under a full optimization of all other internal coordinates of the molecule. The two maximum energy conformations (transition states) of the rotational barrier were then the initial points for the optimization of the transition states using the TS keyword.¹⁹ The influence of the different zero point vibrations (ZPV) and thermal corrections were not considered.

References

- 1 J. Woller, PhD Thesis, Potsdam, 1996.
- 2 K. Pihlaja, P. Oksman, J. Woller, G. Kempter and E. Kleinpeter, unpublished results.
- 3 G. Fischer, W.-D. Rudolf and E. Kleinpeter, *Magn. Reson. Chem.*, 1991, **29**, 212.
- 4 E. Kleinpeter, K. Rasch, W.-D. Rudolf and J. Schmidt, *J. Prakt. Chem.*, 1991, **333**, 131.
- 5 J. Sandström and I. Wennerbeck, *Acta Chem. Scand., Ser. B*, 1970, **24**, 1191.
- 6 Y. Shvo and I. Belsky, *Tetrahedron*, 1969, **25**, 4649.
- 7 I. Belsky, H. Dodiuk and Y. Shvo, *J. Org. Chem.*, 1977, **42**, 2734.
- 8 E. Kleinpeter, St. Thomas, G. Uhlig and W.-D. Rudolf, *Magn. Reson. Chem.*, 1993, **31**, 714.
- 9 H. Shanan-Atidi and K. H. Bar-Eli, *J. Phys. Chem.*, 1970, **74**, 961.
- 10 K. Pihlaja and E. Kleinpeter, *Carbon-13 NMR Chemical Shifts in Structural and Stereochemical Analysis, Methods in Stereochemical Analysis*, ed. A. P. Marchand, VCH Publishers, New York, Weinheim, Cambridge, 1994.
- 11 Also **2**, **3** ($n = 2$, *exo*) decompose at higher temperatures; however, the signals of the decomposition products do not overlap with the H1 signals and the coalescence phenomena could be studied.
- 12 K. Yoshikawa and H. Terada, *J. Am. Chem. Soc.*, 1982, **104**, 7644; A. Safarzadeh-Amiri, *Can. J. Chem.*, 1984, **62**, 1895; Y. Yamamoto, T. Okayima, Y. Fukazawa, T. Fujii, Y. Hata and S. Sawada, *J. Chem. Soc., Perkin Trans. 2*, 1998, 561.
- 13 J. J. P. Stewart, *J. Comput. Chem.*, 1989, **10**, 221.
- 14 SYBYL[®] Molecular Modelling Software, version SYBYL 6.4, TRIPOS Inc.
- 15 J. Baker, *J. Comput. Chem.*, 1986, **7**, 385.
- 16 GAUSSIAN94, Revision E.2, M. J. Frisch, G. W. Trucks, H. B. Schlegel, P. M. W. Gill, B. G. Johnson, M. A. Robb, J. R. Cheeseman, T. Keith, G. A. Petersson, J. A. Montgomery, K. Raghavachari, M. A. Al-Laham, V. G. Zakrzewski, J. V. Ortiz, J. B. Foresman, J. Cioslowski, B. B. Stefanow, A. Nanayakkara, M. Challacombe, C. Y. Peng, P. Y. Ayala, W. Chen, M. W. Wong, J. L. Andres, E. S. Replogle, R. Gomperts, R. L. Martin, D. J. Fox, J. S. Binkley, D. J. Defrees, J. Baker, J. J. P. Stewart, M. Head-Gordon, C. Gonzales and J. A. Pople, Gaussian Inc., Pittsburg, PA, 1995.
- 17 W. J. Hehre, L. Radom, P. v. R. Schleyer and J. A. Pople, *Ab initio Molecular Orbital Theory*, Wiley, New York, 1986.
- 18 C. Peng and H. B. Schlegel, *Israel J. Chem.*, 1993, **33**, 449.
- 19 C. Peng, P. Y. Ayala, H. B. Schlegel and M. J. Frisch, *J. Comput. Chem.*, 1996, **17**, 49.

Paper 8/03732I

Received 18th May 1998

Accepted 22nd June 1998